



Quantum entanglement between a hole spin confined to a semiconductor quantum dot and a photon

Meisam Memarzadeh^{1,a} , Mostafa Sahrai¹, Hamid R. Hamed²

¹ Faculty of Physics, University of Tabriz, Tabriz, Iran

² Institute of Theoretical Physics and Astronomy, Vilnius University, Saulėtekio 3, 10257 Vilnius, Lithuania

Received: 16 January 2022 / Accepted: 2 January 2023

© The Author(s), under exclusive licence to Società Italiana di Fisica and Springer-Verlag GmbH Germany, part of Springer Nature 2023

Abstract We demonstrate quantum entanglement between a single hole spin confined to a positively charged semiconductor quantum dot (QD) and a photon spontaneously emitted from the matter's excited state. The QD system is in the Voigt geometry with two ground hole spin states and two excited trion states. We consider the light-matter coupling initially prepared in one of the ground hole spin states. For very weak Rabi frequencies, the spin-flip process transfers most of the population to another hole spin state, leading to the disentanglement between the single photon and single QD hole spin. A maximum entanglement is achieved by increasing the intensity of Rabi frequencies. In this case, the population almost equally distributes among all the bare quantum states. Our results may pave the way toward creating a scalable QD quantum computing architecture relying on the photon as flying qubits to mediate entanglement between distant nodes of a QD network.

1 Introduction

Quantum entanglement offers unique insights into the fundamental principles of our physical world, while it provides the basis of novel quantum information processing (QIP) protocols, such as quantum teleportation [1], quantum cryptography [2, 3], quantum metrology, sensing, imaging [4] and quantum computing [5–7]. Various host media have been utilized to implement such QIP protocols, including trapped ions and cold atoms [8, 9], superconducting circuits [10, 11], and diamonds [12].

The spin of an individual charge carrier in a semiconductor quantum dot has been identified as a single quantum storage device with fast information processing suitable for different QIP architectures [13–15]. During recent years, there has been a growing interest in demonstration of the spin–photon quantum entanglement based on a single electron spin confined to a negatively charged quantum dot (QD) [16–19]. The spin of a single electron in a QD is a natural two-level system that can effectively serve as a qubit for quantum information processing [20, 21]. However, the electrons interact with their environment and quickly lose their coherence properties. As a result, the electron spin represents rather small coherence times, because of the strong hyperfine interaction with the nuclear spin bath in the QD [22, 23]. The conduction band wave-function consists of atomic S-orbitals and therefore exhibits large amplitude at each individual nucleus [24].

A single heavy-hole (HH) spin provides a practicable alternative to avoid decoherence by extending the coherence properties [25, 26]. A main reason for such a long lived coherence of the holes compared to the electrons is due to the difference in the hyperfine interaction [27, 28]. The valence band is constructed from atomic P-orbitals. The hole spin wave functions have a vanishing amplitude at the location of each nucleus of QD, making the hyperfine interaction for the HH much weaker than the electron [29].

One can introduce a relation for the decoherence time as $\frac{1}{T_2} = \frac{1}{2T_1} + \frac{1}{T_2^*}$ [30], in which T_1 , T_2 and T_2^* represent the spin relaxation time, decoherence time and the dephasing time, respectively. It should be pointed out that the spin relaxation time T_1 indicates the time of a spin-flip ($|\uparrow\rangle \rightarrow |\downarrow\rangle$) process due to spin interactions with the environment. The decoherence time T_2 describes the lifetime of quantum superposition of spin up and spin down states ($|\uparrow\rangle + |\downarrow\rangle$). For the electron and the hole, this time has been reported to be about $T_2 = 3 \mu\text{s}$ [31, 32] and $T_2 = 0.4 \pm 0.2 \mu\text{s}$ [33], respectively. Finally, the dephasing time T_2^* represents the decoherence time for an ensemble measurement (the time average coherence). Dephasing time plays an important role in studying the spin-photon entanglement. The longer is this time, the stronger is the entanglement in the system. For the electron spin states, this time is of the order of few nanometers 1–10 ns [34], while for the hole spin states, it is equal to 100 ns [29, 35]. This indicates that as compared to an electron spin, a HH spin improves the coherence of the system, enabling the study of quantum entanglement generation in a deterministic regime.

In this work, we investigate the spin-photon entanglement of a four-level hole spin state light-matter coupling in the presence of an in-plane magnetic field at a positively charged self-assembled QD. In order to investigate the spin-photon entanglement, we

^a e-mail: m.memarzadeh@tabrizu.ac.ir (corresponding author)

use the Von Neumann entropy to determine the degree of entanglement (DEM) [36–38]. The concept of entropy plays a key role in statistical mechanics and information theory. To describe the state of a physical system in quantum mechanics, there is uncertainty in its details, which is measured by the entropy. In quantum mechanics, the Von Neumann entropy provides a good measurement over the information. Quantum information can be described based on quantum statistics. Entropy measures the uncertainty associated with a probability distribution (classical and quantum). In quantum entanglement, information can be shared between entangled systems. During this process, we will lose some information as we do not have access to the exact information in each system. Such uncertainty in the information of the subsystems is in common between entanglement and entropy. This indicates that calculating the entropy for one of the subsystems provides a good measure of entanglement. We investigate the spin-photon entanglement behaviors by applying laser fields to the quantum dot system. In this case, the hole spin states, as well as the spontaneous emission (photons), are the two main subsystems. There is no interaction initially between the field and the matter; hence, the total entropy, as well as the entropy of each subsystem, is zero. As a result, the system will remain in a pure state. After applying laser fields to the system, the entropy of the whole system will remain zero, yet the reduced entropy of each subsystem (spin and photon) will be modified due to the interaction between them. As the reduced entropy increases, the information is lost from each of the subsystems, implying that the two subsystems act as a single system (the so-called entangled system). In other words, the entanglement of subsystems increases with the increase in entropy. Therefore, any change in the entropy can provide a good measure over the degree of entanglement between quantum subsystems. The light emitted after interacting with the quantum dot contains its information as it is entangled with the spin states of the quantum system.

2 Model and equations

Let us consider a single-charged InAs/GaAs self-assembled QD with a Z-axis growth direction which is charged by a single hole. Figure 1a shows the allowed optical transitions in a positively charged QD in the absence of a magnetic field. The ground hole spin states are labeled as $|1\rangle \equiv |\downarrow\rangle_z$ and $|2\rangle \equiv |\uparrow\rangle_z$, while the two excited trion states are determined by $|3\rangle \equiv |\uparrow\downarrow, \uparrow\rangle_z$ and $|4\rangle \equiv |\uparrow\downarrow, \downarrow\rangle_z$. Here, \uparrow (\downarrow) and \uparrow (\downarrow) denote a HH and an electron with spins parallel (antiparallel) to the z-axis, respectively. The trion spin state $|J, J_z\rangle$ consists of two heavy-holes with spins in opposite directions and an unpaired electron, in particular for heavy-hole states in trion, one has $|J = \frac{3}{2}, J_z = \pm\frac{3}{2}\rangle$ [29]. Due to optical selection rules, only $|2\rangle \leftrightarrow |3\rangle$ and $|1\rangle \leftrightarrow |4\rangle$ transitions can be driven by the circularly polarized laser field (σ^+ , σ^-) and the diagonal transitions $|1\rangle \leftrightarrow |3\rangle$ and $|2\rangle \leftrightarrow |4\rangle$ are not permitted. When an external magnetic field is applied along the x-axis or perpendicular to the growth direction (the so-called Voigt geometry), more suitable states are created, as in this case, the ‘cross’ transitions are allowed (Fig. 1b). The magnetic field (B_x) has now mixed the hole and trion states, and the Zeeman effect separates the resulting eigenstates by $\Delta_h = g_{h,x}\mu_B B_x$ and $\Delta_e = g_{e,x}\mu_B B_x$. Note that, here, μ_B shows the Bohr magneton and $g_{h,x(e,x)}$ stands for the Lande factor of the hole (electron). Therefore, the new eigenstates of the system (x-basis states) are (after transformation from circular basis to the linear superposition):

$$\begin{aligned} |1\rangle \equiv |\downarrow\rangle_x &= \frac{1}{\sqrt{2}}(|\uparrow\rangle_z - |\downarrow\rangle_z) & |2\rangle \equiv |\uparrow\rangle_x &= \frac{1}{\sqrt{2}}(|\uparrow\rangle_z + |\downarrow\rangle_z) \\ |3\rangle \equiv |\uparrow\downarrow, \uparrow\rangle_x &= \frac{1}{\sqrt{2}}(|\uparrow\downarrow, \uparrow\rangle_z + |\uparrow\downarrow, \downarrow\rangle_z) & |4\rangle \equiv |\uparrow\downarrow, \downarrow\rangle_x &= \frac{1}{\sqrt{2}}(|\uparrow\downarrow, \uparrow\rangle_z - |\uparrow\downarrow, \downarrow\rangle_z) \end{aligned} \quad (1)$$

Figure 1b illustrates the energy-level diagram of such a four-level light-matter coupling. A linear y-polarized laser acts on the ‘cross’ transitions of the new level diagram, while an x-polarized laser couples the ‘vertical’ transitions. Because the transitions are linearly polarized, one can easily describe the electric field as

$$\mathbf{E}(t) = \frac{1}{2}(E_x(t)\hat{x} + E_y(t)\hat{y})e^{-i\omega t} + \frac{1}{2}(E_x^*(t)\hat{x} + E_y^*(t)\hat{y})e^{i\omega t}. \quad (2)$$

The Hamiltonian including the effect of the magnetic field of the system reads

$$H = H_0 + V_{\text{Zeeman}}, \quad (3)$$

where H_0 is the free energy of the QD, i.e., in the absence of magnetic and optical fields, while [39]

$$V_{\text{Zeeman}} = g_e\mu_B B \hat{S}_{e,x} - g_h\mu_B B \hat{S}_{h,x}, \quad (4)$$

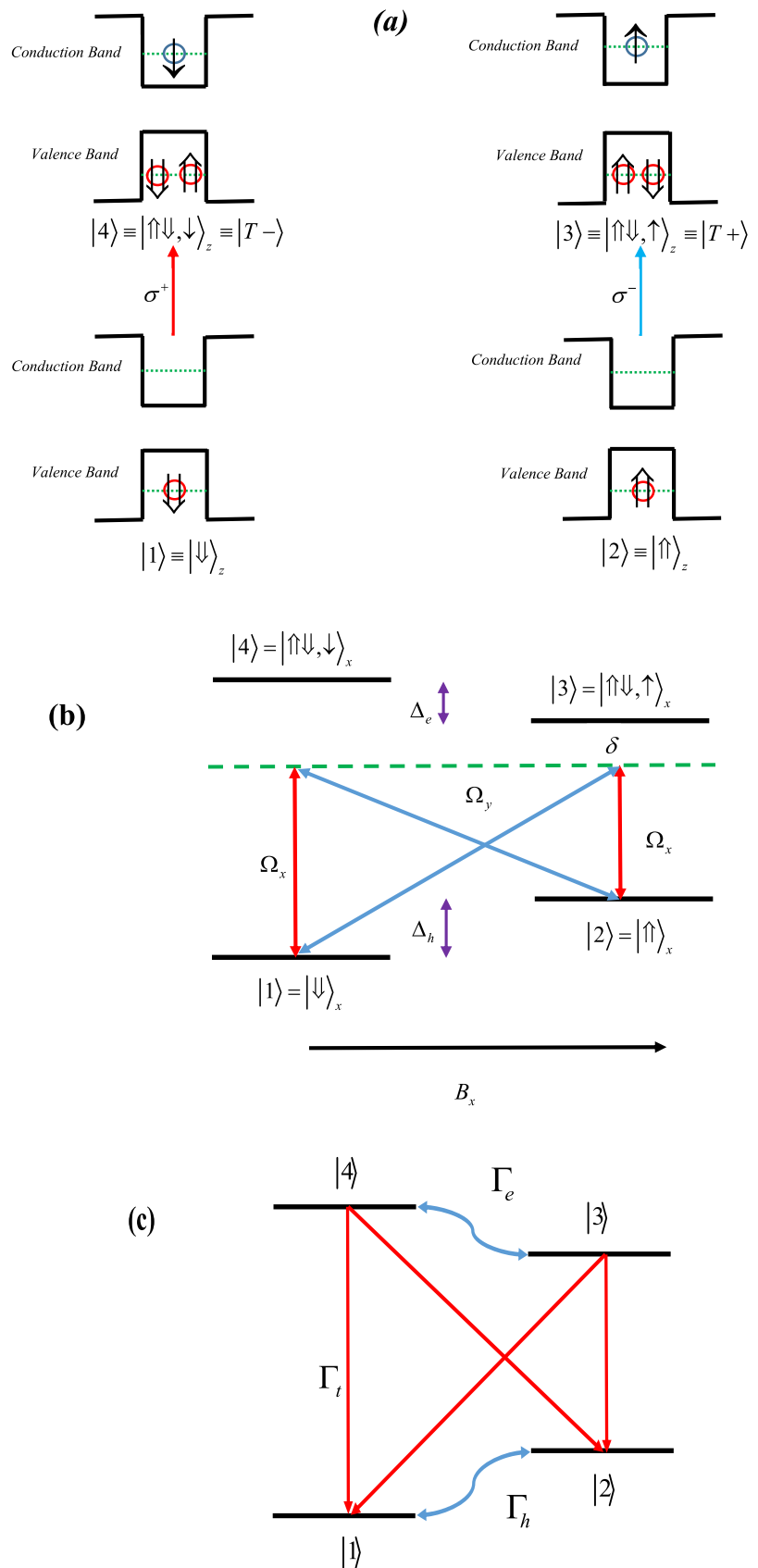
denotes the interaction Hamiltonian of the electron and hole with the magnetic field aligned in the x-direction. Note that, here, $\hat{S}_{e,x}$ and $\hat{S}_{h,x}$ are the spin operators for the electron and hole, respectively.

In order to calculate the optically allowed transitions in the proposed configuration, we need to write the Hamiltonian for optical interactions (H_{optical}) as

$$\langle i|H_{\text{optical}}|j\rangle = \langle i|H_0|j\rangle + \langle i|V_{\text{optical}}|j\rangle = \langle E_i\delta_{i,j}\rangle + \langle i|V_{\text{optical}}|j\rangle. \quad (5)$$

In the dipole approximation, one has $V_{\text{optical}} = -\boldsymbol{\mu}\cdot\mathbf{E} = e\mathbf{r}\cdot\mathbf{E}$, where e is a positive number giving the magnitude of an electron’s charge. Since \mathbf{E} does not operate upon the state vectors, it is sufficient to evaluate $e\langle i|\mathbf{r}|j\rangle$ to determine the optically allowed

Fig. 1 **a** The four z -basis eigenstates and allowed transition of a positively charged QD in the absence of a magnetic field. σ_+ (σ_-) is the right (left)-handed optical polarization that satisfies the optical selection rule. **b** Energy-level structure and allowed optical transitions for a charged QD in presence of the magnetic field which is oriented in the x -direction (Voigt geometry). **c** Schematic of the decay rate in four spin levels of singly charged QD



transitions and their polarization selection rules. By considering the irreducible spherical tensors ($\mathbf{r} = -r_{-1}\epsilon_{+1} - r_{+1}\epsilon_{-1} + r_0\epsilon_0$ where $\epsilon_{\pm 1} = \mp \frac{(\hat{x} \pm i\hat{y})}{\sqrt{2}}$, $\epsilon_0 = \hat{z}$), the selection rules for optical transitions can be expressed as [39]

$$\begin{aligned} e(4|r|1) &\equiv -\frac{\delta}{\sqrt{2}}\hat{x}, & e(3|r|2) &\equiv -\frac{\delta}{\sqrt{2}}\hat{x}, \\ e(3|r|1) &\equiv -\frac{\delta}{\sqrt{2}}i\hat{y}, & e(4|r|2) &\equiv -\frac{\delta}{\sqrt{2}}i\hat{y}. \end{aligned} \quad (6)$$

The Hamiltonian for the system in the Voigt geometry becomes

$$H = \begin{pmatrix} \frac{\hbar}{2}(\omega_0 - \Delta_h) & V_{12} & V_{13} & V_{14} \\ V_{21} & \frac{\hbar}{2}(\omega_0 + \Delta_h) & V_{23} & V_{24} \\ V_{31} & V_{32} & \frac{\hbar}{2}(-\omega_0 - \Delta_e) & V_{34} \\ V_{41} & V_{42} & V_{43} & \frac{\hbar}{2}(-\omega_0 + \Delta_e) \end{pmatrix}. \quad (7)$$

Based on the interaction of the electric and magnetic fields given in Eqs. (2)–(4) with quantum dot featured in Fig. 1b, in a proper rotating frame, Eq. (7) can be written as

$$H_F = \begin{pmatrix} \frac{\hbar}{2}(\delta - \Delta_h) & V_{12} & V_{13}e^{-i\omega t} & V_{14}e^{-i\omega t} \\ V_{21} & \frac{\hbar}{2}(\delta + \Delta_h) & V_{23}e^{-i\omega t} & V_{24}e^{-i\omega t} \\ V_{31}e^{i\omega t} & V_{32}e^{i\omega t} & -\frac{\hbar}{2}(\delta + \Delta_e) & V_{34} \\ V_{41}e^{i\omega t} & V_{42}e^{i\omega t} & V_{43} & \frac{\hbar}{2}(-\delta + \Delta_e) \end{pmatrix}, \quad (8)$$

where $\delta = \omega_0 - \omega$. Note that, ω_0 represents the average transition frequency of two levels $|i\rangle$ and $|j\rangle$ and is about $5.7 \pm 0.2 \mu\text{ev}$ [26].

Using rotating wave approximation (RWA), Eq. (8) can be expressed as (see Appendix).

$$H_{F,RWA} = \frac{\hbar}{2} \begin{pmatrix} -\delta - \Delta_h & 0 & \Omega_y^* & \Omega_x^* \\ 0 & -\delta + \Delta_h & \Omega_x^* & \Omega_y^* \\ \Omega_y & \Omega_x & \delta - \Delta_e & 0 \\ \Omega_x & \Omega_y & 0 & \delta + \Delta_e \end{pmatrix}. \quad (9)$$

Next, we are interested in the time evolution of the system using the Lindblad equation

$$\dot{\rho} = \frac{-i}{\hbar} [H_{F,RWA}, \rho] + \mathcal{L}(\rho) \quad (10)$$

where ρ denotes the density matrix elements. Here, $\mathcal{L}(\rho)$ is the Liouvillian operator describing the total relaxation processes. Using Hamiltonian $H_{F,RWA}$ featured in Eqs. (9) and (10), the density matrix elements describing the evolution of quantum system can be obtained as

$$\begin{aligned} \dot{\rho}_{11} &= \frac{i}{2} (\rho_{14}\Omega_x + \rho_{13}\Omega_y - \rho_{31}\Omega_y^* - \rho_{41}\Omega_x^*) + \frac{\Gamma_t}{2} (\rho_{44} + \rho_{33}) + \Gamma_h (\rho_{22} - \rho_{11}), \\ \dot{\rho}_{22} &= \frac{i}{2} ((\rho_{23} + \rho_{24})\Omega_x - \rho_{42}\Omega_y^* - \rho_{32}\Omega_x^*) + \frac{\Gamma_t}{2} (\rho_{44} + \rho_{33}) + \Gamma_h (\rho_{11} - \rho_{22}), \\ \dot{\rho}_{33} &= -\frac{i}{2} (\rho_{13}\Omega_y + \rho_{23}\Omega_x - \rho_{31}\Omega_y^* - \rho_{32}\Omega_x^*) - \Gamma_t \rho_{33} + \Gamma_e (\rho_{44} - \rho_{33}), \\ \dot{\rho}_{44} &= -\frac{i}{2} ((\rho_{14} + \rho_{24})\Omega_x - \rho_{42}\Omega_y^* - \rho_{41}\Omega_x^*) - \Gamma_t \rho_{44} + \Gamma_e (\rho_{33} - \rho_{44}), \\ \dot{\rho}_{12} &= \frac{i}{2} (2\Delta_h \rho_{12} + (\rho_{13} + \rho_{14})\Omega_x - \rho_{32}\Omega_y^* - \rho_{42}\Omega_x^*) - \gamma_h \rho_{12}, \\ \dot{\rho}_{13} &= \frac{i}{2} ((2\delta + \Delta_h - \Delta_e)\rho_{13} + (\rho_{11} - \rho_{33})\Omega_y^* + (\rho_{12} - \rho_{43})\Omega_x^*) - \gamma_t \rho_{13}, \\ \dot{\rho}_{14} &= \frac{i}{2} ((2\delta + \Delta_e + \Delta_h)\rho_{14} + (\rho_{12} - \rho_{34})\Omega_y^* + (\rho_{11} - \rho_{44})\Omega_x^*) - \gamma_t \rho_{14}, \\ \dot{\rho}_{23} &= \frac{i}{2} ((2\delta - \Delta_e - \Delta_h)\rho_{23} + (\rho_{21} - \rho_{43})\Omega_y^* + (\rho_{22} - \rho_{33})\Omega_x^*) - \gamma_t \rho_{23}, \\ \dot{\rho}_{24} &= \frac{i}{2} ((2\delta - \Delta_h + \Delta_e)\rho_{24} + (\rho_{22} - \rho_{44})\Omega_y^* + (\rho_{21} - \rho_{34})\Omega_x^*) - \gamma_t \rho_{24}, \\ \dot{\rho}_{34} &= \frac{i}{2} (2\Delta_e \rho_{34} - \rho_{14}\Omega_x - \rho_{24}\Omega_y + \rho_{32}\Omega_x^* + \rho_{31}\Omega_y^*) - \gamma_e \rho_{34}. \end{aligned} \quad (11)$$

Here, Γ_t is the decay rate of trion states (in fact Γ_t represents recombination of electron–hole), Γ_h (Γ_e) denotes the spin-flip rate for the hole (electron) and γ_i indicates decoherence rate (Fig. 1c). The corresponding detuning between the laser pulse and

the QD transitions is denoted by δ . Consider the QD and its spontaneous emission photon as a bipartite system with S (spin of the QD system) and P (photon) as subsystems. Assume the density operator ρ_{SP} that describes this two-part (spin-photon) system. The system is entangled if ρ_{SP} cannot be written as a tensor product of two systems ($\rho_{SP} \neq \rho_S \otimes \rho_P$). To measure the degree of entanglement (DEM) between the QD and photon, we use the Von Neumann entropy

$$S = -Tr(\rho \ln \rho). \tag{12}$$

Araki and Lieb proposed an inequality that links the entropy of the subsystems [40]

$$|S_S(t) - S_P(t)| \leq S_{SP}(t) \leq |S_S(t) + S_P(t)|, \tag{13}$$

where $S_{SP}(t) = -Tr(\rho_{SP} \ln \rho_{SP})$ is the total entropy of the spin-photon system. We assume that the spin-photon system is initially in a pure state, therefore, to determine the degree of entanglement, we just need to calculate the QD entropy $\rho_S(t)$.

Finally, the DEM can be presented in terms of eigenvalues ($\lambda_{S(P)}$) of the reduced density matrix as

$$DEM = S_S(t) = S_P(t) = -\sum_{i=1}^4 \lambda_i \ln \lambda_i(t). \tag{14}$$

3 Results and discussion

In order to study the entanglement numerically in this section, we solve simultaneously the density matrix equations of the motion given in Eqs. (11) and (14). The maximum degree of entanglement can be obtained by means of the relation $\text{Max}(DEM) = \log_2 [\min(d_S, d_P)]$, in which d_S and d_P are the dimensions of Hilbert space related to the subsystems. According to the number of spin states available, the maximum entanglement rate for this system is ($DEM = 2$).

Figure 2(a) shows how the entanglement changes when the Rabi frequency varies in the steady-state condition. For the steady-state response of Eqs. (11), we set $\Omega_x = 1.75\Omega_y$, $\delta = 2 \mu\text{eV}$ and plot the DEM and population distributions against Ω_x . Other parameters are $\Gamma_e = 0.0009 \mu\text{eV}$, $\Gamma_h = 0.000671 \mu\text{eV}$, $\Gamma_l = 0.5 \mu\text{eV}$, $\Delta_e = 5 \mu\text{eV}$, and $\Delta_h = 9 \mu\text{eV}$. In all simulations, we have assumed the case in absence of the pure dephasing, i.e., $\gamma_l = \frac{\Gamma_l}{2}$, $\gamma_e = \Gamma_e$ and $\gamma_h = \Gamma_h$. One can see that an increase in the Rabi frequency results in an increase in the entanglement of the system. The DEM is quite small at very low frequencies when most of the population is distributed in the state $|1\rangle$. The situation improves for larger Rabi frequencies as the population starts to be distributed in all four states. However, a dip appears in the entanglement profile around $\Omega_x = 10 \mu\text{eV}$. The population distribution also experiences a divergence at the same Rabi frequency range, i.e., around $\Omega_x = 10 \mu\text{eV}$. The entanglement increases and becomes stable for larger frequencies $\Omega_x > 10 \mu\text{eV}$. In this case, the population is equally distributed in all levels, each containing almost a quarter of the total population. (Fig. 2b).

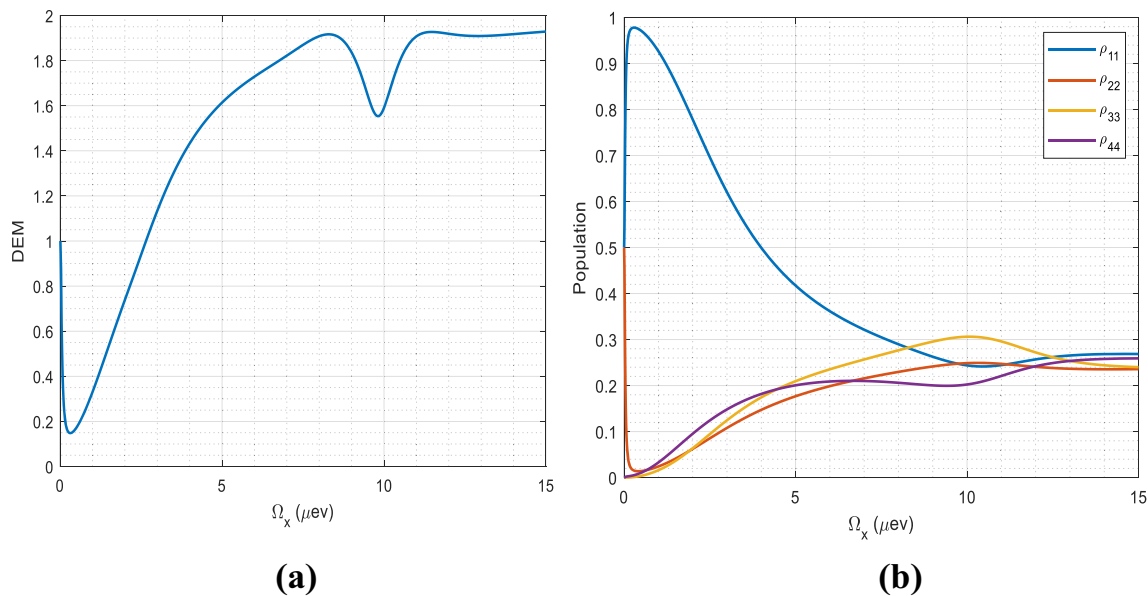


Fig. 2 Plots of the **a** DEM and **b** population distribution versus the Rabi frequency ($\Omega_x = 1.75\Omega_y$). The selected parameters are $\Gamma_e = 0.0009 \mu\text{eV}$, $\Gamma_h = 0.000671 \mu\text{eV}$, $\Gamma_l = 0.5 \mu\text{eV}$, $\delta = 2 \mu\text{eV}$, $\Delta_e = 5 \mu\text{eV}$, $\Delta_h = 9 \mu\text{eV}$. We have assumed a case in the absence of pure dephasing, i.e., $\gamma_l = \frac{\Gamma_l}{2}$, $\gamma_e = \Gamma_e$, and $\gamma_h = \Gamma_h$ [26]

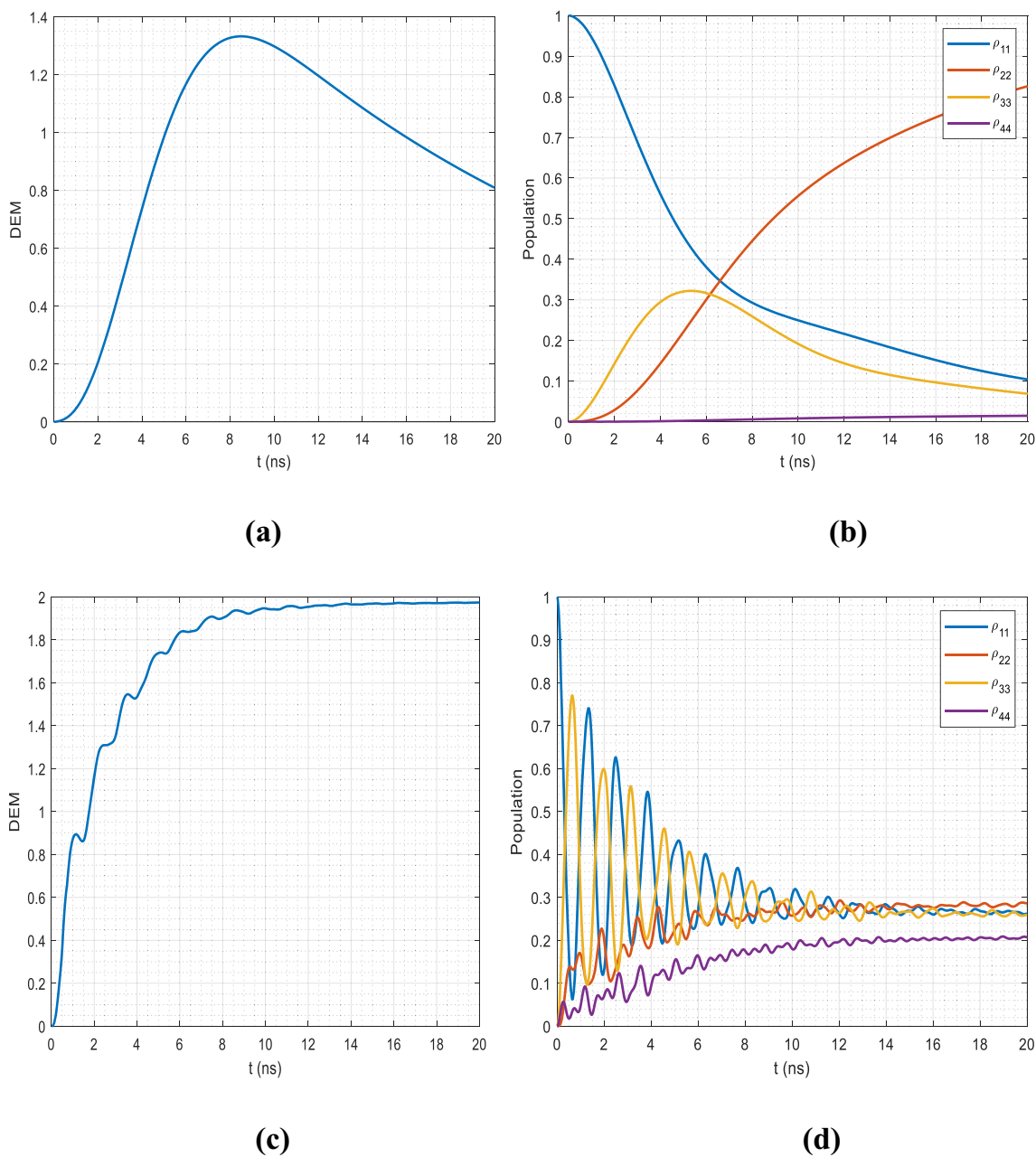


Fig. 3 Temporal behavior of **a, c** DEM and population distribution **b, d** for different values of Rabi frequencies **a, b** $\Omega_x = \Omega_y = 0.5 \mu\text{eV}$ and **c, d** $\Omega_x = 5 \mu\text{eV}, \Omega_y = 3 \mu\text{eV}$. Other parameters are the same as Fig. 2

As we mentioned for the maximally entangled state, the DEM is given by $\text{DEM} = \log_2[\min(d_S, d_P)]$. Four QD eigenvalues lead to $\text{DEM} = 2$ as it is depicted in Fig. 2a. If this DEM describes a (maximally) mixed subsystem, then the whole pure state is (maximally) entangled. To distinguish pure, mixed and maximally mixed states, a real and positive parameter known as purity of the state χ is introduced as $\mu(\chi) = \text{Tr}(\chi^2)$. In the case of an n-dimensional state, we find $\frac{1}{n} \leq \mu(\chi) \leq 1$. For $\mu(\chi) = 1$, $\frac{1}{n} < \mu(\chi) < 1$ and $\mu(\chi) = \frac{1}{n}$, the state is pure, mixed and maximally mixed, respectively. We observe that by increasing the Rabi frequency, the population distribution of all the states becomes almost equal. In this case, all the coherence terms are zero, and the ρ_S will be diagonal that can be written as $\rho_S = \frac{1}{4}\hat{I}$, where $\frac{1}{4}$ and \hat{I} are the population of each level and the identity matrix, respectively. Here, $\mu(\chi) = \frac{1}{4}$, then ρ_S describes a maximally mixed state. Thus, the whole system is in the maximally entangled state. However, for $\Omega_x = 10 \mu\text{eV}$, the population distribution of four presented levels is not equal, and the off-diagonal terms are not zero leading to reduction in the entanglement.

Next, we assume that the QD system is prepared in its ground state ($\rho_{11}(0) = 1$). This assures that the system has been initially populated in a pure state. In such a situation, the entropy of the spin states ($S_S(t)$) provides a sufficient tool to calculate the degree

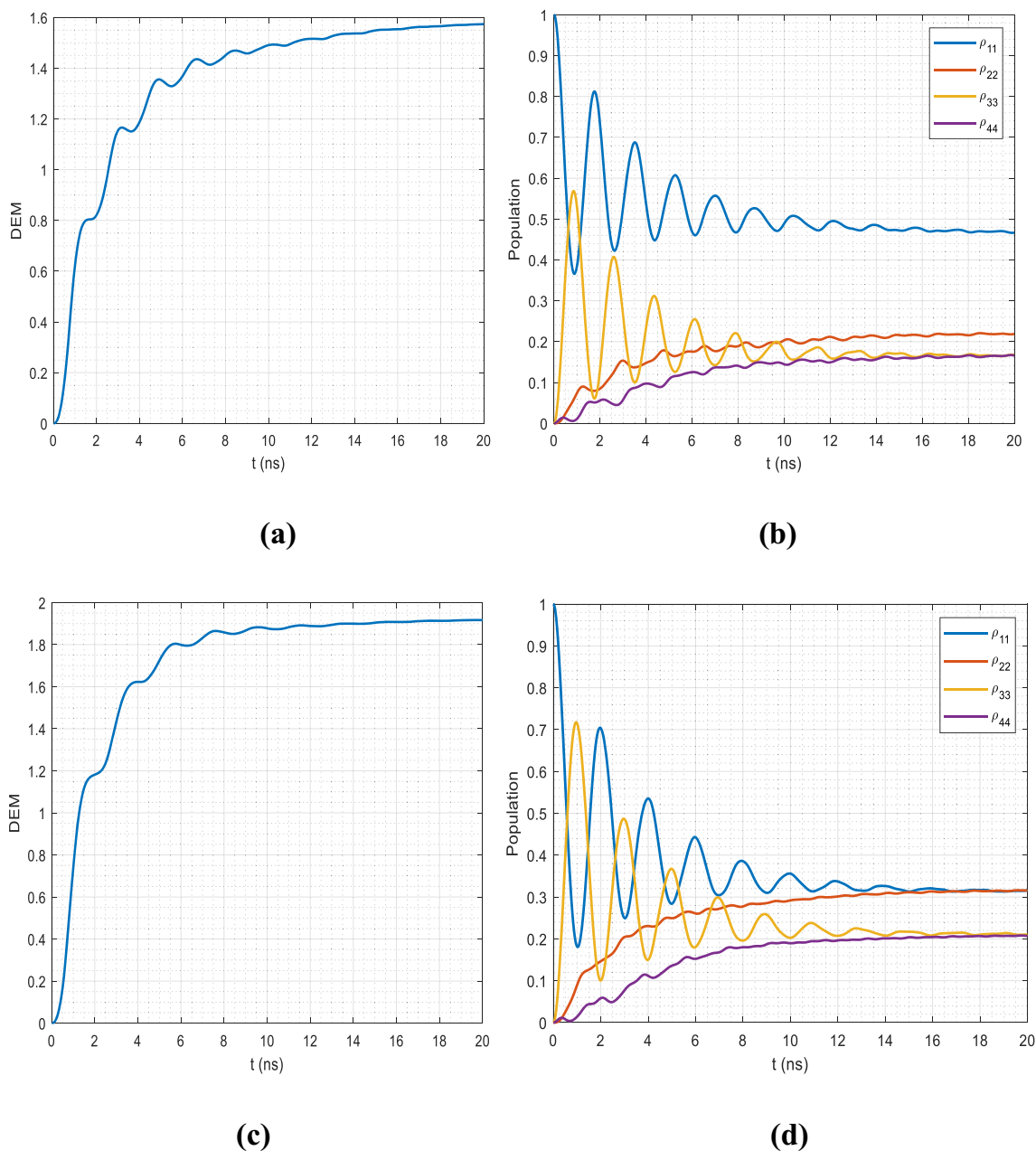


Fig. 4 Temporal behavior of **a, c** DEM and population distribution **b, d** for different values of the detuning **a, b** $\delta = 0$, and **c, d** $\delta = 1 \mu\text{eV}$. Here, $\Omega_x = 3 \mu\text{eV}$, $\Omega_y = 1 \mu\text{eV}$ and the other parameters are the same as Fig. 2

of entanglement of the bipartite (hole spin + photon) system. We assume the non-resonance condition $\delta = 2 \mu\text{eV}$ and illustrate in Fig. 3a the time evolution of spin-photon entanglement for different values of Rabi frequencies.

For the four-level QD system initially prepared in its ground state $|1\rangle$ and for the weak Rabi frequencies $\Omega_x = \Omega_y = 0.5 \mu\text{eV}$, one can see from Fig. 3a that an initially zero DEM slowly rises to a maximum value and then starts to decline. No steady-state DEM value is obtained in this case. Such a reduction in the DEM causes the subsystems to lose the entanglement. As can be observed in Fig. 3b, as time increases, the system initially prepared in its ground level $|1\rangle$ transfers most of the population to the lower spin level $|2\rangle$. In this case, the population of level $|4\rangle$ is strongly suppressed. This is due to the weak optical pumping ($\Omega_x = \Omega_y = 0.5 \mu\text{eV}$) which cannot excite most of the population from the ground state $|1\rangle$ to the trion states $|3\rangle$ and $|4\rangle$. On the other hand, trion states decay with a rate Γ_t to both lower levels $|1\rangle$ and $|2\rangle$ with an equal probability. Once the dot decays to the spin state $|1\rangle$, it cannot be trapped in this state, as the spin-flip occurs transferring the population to the lower level $|2\rangle$. As a result, most of the population will be distributed in the spin state $|2\rangle$. This reduces the entropy and makes the subsystems disentangled.

Setting $\Omega_x = 5 \mu\text{eV}$ and $\Omega_y = 3 \mu\text{eV}$ improves the situation as illustrated in Fig. 3c. One can see that at the early time, the DEM is zero indicating no entanglement between the light and matter. As time increases, entanglement oscillates and rises to its maximum steady-state value. This implies a strong entanglement between the single hole spin confined to the single-charged semiconductor quantum dot and the photon spontaneously emitted from the quantum dot's excited state. In order to elucidate the physics behind such a strong spin-photon entanglement, we plot in Fig. 3d the temporal distribution of population. Clearly, the population is now more uniformly distributed in all spin states due to the contribution of strong optical pumping, as well as the spin-flip effect. This causes an increase in the entropy of the system, leading to a remarkable growth of the steady-state DEM.

Figure 4 illustrates the effect of detuning on DEM and population. For the resonance condition $\delta = 0$, most of the population remains in the first lower level (Fig. 4b), yielding a low entanglement (Fig. 4a). Setting $\delta = 1 \mu\text{eV}$, the entanglement increases significantly, as can be seen in (Fig. 4c). In this case, the population is relatively distributed between all four levels.

4 Conclusions

In summary, we investigate the generation of entanglement between the spin states of a single hole in a self-assembled quantum dot and its spontaneous emission. The quantum dot, which is charged with a hole, is excited by a linearly polarized laser field in the presence of a magnetic field in the Voigt geometry. It has been shown that a strong entanglement can be generated between the spin and photon. Such a high degree of entanglement suggests an attractive platform for creating a powerful quantum interface [41].

Data Availability Statement This manuscript has associated data in a data repository. [Authors' comment: The datasets generated during and/or analyzed during the current study are available from the corresponding author on reasonable request.]

Appendix

As an example, we calculate the term H_{14} in Eq. (9). From Eqs. (2), (6) and (7), one can evaluate the Hamiltonian term

$$\begin{aligned} V_{14} &= -1|\mu|4.\mathbf{E}(t) = -\frac{\wp}{2\sqrt{2}}\left(E_x(t)e^{-i\omega t} + E_x^*(t)e^{i\omega t}\right) \\ &= \frac{\hbar}{2}\left(\Omega_x(t)e^{-i\omega t} + \Omega_x^*(t)e^{i\omega t}\right), \end{aligned}$$

where $\Omega_x \equiv \frac{\wp E_x}{\hbar\sqrt{2}}$ and $\Omega_y \equiv \frac{i\wp E_y}{\hbar\sqrt{2}}$ are the Rabi frequencies along the x - and y -axis.

Thus,

$$H_{14} = V_{14}e^{-i\omega t} = \frac{\hbar}{2}\left(\Omega_x(t)e^{-2i\omega t} + \Omega_x^*(t)\right). \quad (\text{A1})$$

According to the RWA, we can neglect terms that oscillate at 2ω , as they will average out to zero, while the other terms remain unchanged. Therefore, $H_{14} = \frac{\hbar}{2}\Omega_x^*(t)$. Similarly, the other terms of Eq. (9) can be obtained.

References

1. C.H. Bennett, G. Brassard, C. Crépeau, R. Jozsa, A. Peres, W.K. Wootters, Teleporting an unknown quantum state via dual classical and Einstein–Podolsky–Rosen channels. *Phys. Rev. Lett.* **70**, 1895 (1993)
2. A.K. Ekert, Quantum cryptography based on Bell's theorem. *Phys. Rev. Lett.* **67**, 661 (1991)
3. J. Yin, Y.-H. Li, S.-K. Liao, M. Yang, Y. Cao, L. Zhang, J.-G. Ren, W.-Q. Cai, W.-Y. Liu, S.-L. Li, R. Shu, Y.-M. Huang, L. Deng, L. Li, Q. Zhang, N.-L. Liu, Y.-A. Chen, C.-Y. Lu, X.-B. Wang, F. Xu, J.-Y. Wang, C.-Z. Peng, A.K. Ekert, J.-W. Pan, Entanglement-based secure quantum cryptography over 1,120 kilometres. *Nature* **582**, 501 (2020)
4. J.P. Dowling, K.P. Seshadreesan, Quantum optical technologies for metrology, sensing, and imaging. *J. Lightwave Technol.* **33**, 2359 (2015)
5. R. Jozsa, N. Linden, On the role of entanglement in quantum-computational speed-up. *Proc. R. Soc. Lond. Ser. A Math. Phys. Eng. Sci.* **459**, 211 (2003)
6. T.D. Ladd, F. Jelezko, R. Laflamme, Y. Nakamura, C. Monroe, J.L. O'Brien, Quantum computers. *Nature* **464**, 45 (2010)
7. C. Kloeffel, D. Loss, Prospects for spin-based quantum computing in quantum dots. *Annu. Rev. Condens. Matter Phys.* **4**, 51 (2013)
8. R. Blatt, D. Wineland, Entangled states of trapped atomic ions. *Nature* **453**, 1008 (2008)
9. J.J. García-Ripoll, P. Zoller, J.I. Cirac, Quantum information processing with cold atoms and trapped ions. *J. Phys. B At. Mol. Opt. Phys.* **38**, S567 (2005)
10. R. Barends, J. Kelly, A. Megrant, A. Veitia, D. Sank, E. Jeffrey, T.C. White, J. Mutus, A.G. Fowler, B. Campbell, Y. Chen, Z. Chen, B. Chiaro, A. Dunsworth, C. Neill, P. O'Malley, P. Roushan, A. Vainsencher, J. Wenner, A.N. Korotkov, A.N. Cleland, J.M. Martinis, Superconducting quantum circuits at the surface code threshold for fault tolerance. *Nature* **508**, 500 (2014)
11. N. Roch, M.E. Schwartz, F. Motzoi, C. Macklin, R. Vijay, A.W. Eddins, A.N. Korotkov, K.B. Whaley, M. Sarovar, I. Siddiqi, Observation of measurement-induced entanglement and quantum trajectories of remote superconducting qubits. *Phys. Rev. Lett.* **112**, 170501 (2014)
12. K.C. Lee, M.R. Sprague, B.J. Sussman, J. Nunn, N.K. Langford, X.-M. Jin, T. Champion, P. Michelberger, K.F. Reim, D. England, D. Jaksch, I.A. Walmsley, Entangling macroscopic diamonds at room temperature. *Science* (80-) **334**, 1253 (2011)

13. W.B. Gao, A. Imamoglu, H. Bernien, R. Hanson, Coherent manipulation, measurement and entanglement of individual solid-state spins using optical fields. *Nat. Photonics* **9**, 363 (2015)
14. A. Imamog, D. Awschalom, G. Burkard, D.P. DiVincenzo, D. Loss, M. Sherwin, A. Small, Quantum information processing using quantum dot spins and cavity QED. *Phys. Rev. Lett.* **83**, 4204 (1999)
15. W. Yao, R.B. Liu, L.J. Sham, Theory of control of the spin-photon interface for quantum networks. *Phys. Rev. Lett.* **95**, 1 (2005)
16. E. Togan, Y. Chu, A.S. Trifonov, L. Jiang, J. Maze, L. Childress, M.V.G. Dutt, A.S. Sørensen, P.R. Hemmer, A.S. Zibrov, M.D. Lukin, Quantum entanglement between an optical photon and a solid-state spin qubit. *Nature* **466**, 730 (2010)
17. J.R. Schaibley, A.P. Burgers, G.A. McCracken, L.M. Duan, P.R. Berman, D.G. Steel, A.S. Bracker, D. Gammon, L.J. Sham, Demonstration of quantum entanglement between a single electron spin confined to an InAs quantum dot and a photon. *Phys. Rev. Lett.* **110**, 1 (2013)
18. K. De Greve, L. Yu, P.L. McMahon, J.S. Pelc, C.M. Natarajan, N.Y. Kim, E. Abe, S. Maier, C. Schneider, M. Kamp, S. Höfling, R.H. Hadfield, A. Forchel, M.M. Fejer, Y. Yamamoto, Quantum-dot spin-photon entanglement via frequency downconversion to telecom wavelength. *Nature* **491**, 421 (2012)
19. S. Sun, E. Waks, Deterministic generation of entanglement between a quantum-dot spin and a photon. *Phys. Rev. A* **90**, 42322 (2014)
20. D. Loss, D.P. Divincenzo, Quantum computation with quantum dots. *Phys. Rev. A* **57**, 120 (1998)
21. M. Atatüre, J. Dreiser, A. Badolato, A. Högele, K. Karrai, A. Imamoglu, Quantum-dot spin-state preparation with near-unity fidelity. *Science (80-)* **312**, 551 (2006)
22. W.A. Coish, D. Loss, Hyperfine interaction in a quantum dot: non-markovian electron spin dynamics. *Phys. Rev. B* **70**, 195340 (2004)
23. W. Yao, R.-B. Liu, L.J. Sham, Theory of electron spin decoherence by interacting nuclear spins in a quantum dot. *Phys. Rev. B* **74**, 195301 (2006)
24. R.J. Warburton, Single spins in self-assembled quantum dots. *Nat. Mater.* **12**, 483 (2013)
25. A. Tartakovskii, Holes avoid decoherence. *Nat. Photonics* **5**, 647 (2011)
26. D. Brunner, B.D. Gerardot, P.A. Dalgarno, G. Wüst, K. Karrai, N.G. Stoltz, P.M. Petroff, R.J. Warburton, A coherent single-hole spin in a semiconductor. *Science (80-)* **325**, 70 (2009)
27. J. Fischer, W.A. Coish, D.V. Bulaev, D. Loss, Spin decoherence of a heavy hole coupled to nuclear spins in a quantum dot. *Phys. Rev. B Condens. Matter Mater. Phys.* **78**, 1 (2008)
28. C. Testelin, F. Bernardot, B. Eble, M. Chamorro, Hole-spin dephasing time associated with hyperfine interaction in quantum dots. *Phys. Rev. B Condens. Matter Mater. Phys.* **79**, 1 (2009)
29. J.H. Prechtel, A.V. Kuhlmann, J. Houel, A. Ludwig, S.R. Valentin, A.D. Wieck, R.J. Warburton, Decoupling a hole spin qubit from the nuclear spins. *Nat. Mater.* **15**, 981 (2016)
30. M. Borhani, V.N. Golovach, D. Loss, Spin decay in a quantum dot coupled to a quantum point contact. *Phys. Rev. B* **73**, 155311 (2006)
31. D. Press, K. De Greve, P.L. McMahon, T.D. Ladd, B. Friess, C. Schneider, M. Kamp, S. Höfling, A. Forchel, Y. Yamamoto, Ultrafast optical spin echo in a single quantum dot. *Nat. Photonics* **4**, 367 (2010)
32. A. Greilich, D.R. Yakovlev, A. Shabaev, A.L. Efros, I.A. Yugova, R. Oulton, V. Stavarache, D. Reuter, A. Wieck, M. Bayer, Mode locking of electron spin coherences in singly charged quantum dots. *Science (80-)* **313**, 341 (2006)
33. L. Huthmacher, R. Stockill, E. Clarke, M. Hugues, C. Le Gall, M. Atatüre, Coherence of a dynamically decoupled quantum-dot hole spin. *Phys. Rev. B* **97**, 1 (2018)
34. X. Xu, B. Sun, P.R. Berman, D.G. Steel, A.S. Bracker, D. Gammon, L.J. Sham, Coherent population trapping of an electron spin in a single negatively charged quantum dot. *Nat. Phys.* **4**, 692 (2008)
35. J. Houel, J.H. Prechtel, A.V. Kuhlmann, D. Brunner, C.E. Kulewicz, B.D. Gerardot, N.G. Stoltz, P.M. Petroff, R.J. Warburton, High resolution coherent population trapping on a single hole spin in a semiconductor quantum dot. *Phys. Rev. Lett.* **112**, 107401 (2014)
36. B. Sangshekan, N. Einali Saghavaz, A. Hamrah Gharamaleki, M. Sahrai, Maximal atom-photon entanglement by the incoherent pumping fields. *Eur. Phys. J. Plus* **134**, 274 (2019)
37. M. Ghaderi Goran Abad, M. Mahmoudi, Atom-photon entanglement near a plasmonic nanostructure. *Eur. Phys. J. Plus* **135**, 352 (2020)
38. Z. Amini Sabegh, R. Amiri, M. Mahmoudi, Spatially dependent atom-photon entanglement. *Sci. Rep.* **8**, 13840 (2018)
39. J.R. Schaibley, Spin-photon Entanglement and quantum optics with single quantum dots, Ph.D. thesis, University of Michigan, Michigan (2013)
40. H. Araki, E.H. Lieb, Entropy inequalities. *Commun. Math. Phys.* **18**, 160 (1970)
41. K.L. Truex, Optical coherent control of a single charged indium arsenide quantum dot. Ph.D. thesis. University of Michigan, Michigan (2013)

Springer Nature or its licensor (e.g. a society or other partner) holds exclusive rights to this article under a publishing agreement with the author(s) or other rightsholder(s); author self-archiving of the accepted manuscript version of this article is solely governed by the terms of such publishing agreement and applicable law.